Published online 12 December 2019

Nucleic Acids Research, 2020, Vol. 48, No. 4 ***1925–1940***
doi: 10.1093/nar/gkz1175

APE1 senses DNA single-strand breaks for repair and signaling

Yunfeng Lin†, Jude Raj†, Jia Li, Anh Ha, Md. Akram Hossain, Christine Richardson, Pinku Mukherjee and Shan Yan*

Department of Biological Sciences, University of North Carolina at Charlotte, Charlotte, NC 28223, USA

Received September 15, 2019; Revised December 02, 2019; Editorial Decision December 04, 2019; Accepted December 05, 2019

ABSTRACT

DNA single-strand breaks (SSBs) represent the most abundant type of DNA damage. Unrepaired SSBs impair DNA replication and transcription, leading to cancer and neurodegenerative disorders. Although PARP1 and XRCC1 are implicated in the SSB repair pathway, it remains unclear how SSB repair and SSB signaling pathways are coordinated and regulated. Using *Xenopus* egg extract and *in vitro* reconstitution systems, here we show that SSBs are first sensed by APE1 to initiate 3′–5′ SSB end resection, followed by APE2 recruitment to continue SSB end resection. Notably, APE1's exonuclease activity is critical for SSB repair and SSB signaling pathways. An APE1 exonuclease-deficient mutant identified in somatic tissue from a cancer patient highlighted the significance of APE1 exonuclease activity in cancer etiology. In addition, APE1 interacts with APE2 and PCNA, although PCNA is dispensable for APE1's exonuclease activity. Taken together, we propose a two-step APE1/APE2-mediated mechanism for SSB end resection that couples DNA damage response with SSB repair in a eukaryotic system.

INTRODUCTION

Representing ∼10% of all DNA lesions in a genome, DNA single-strand breaks (SSBs) are constantly generated due to oxidative stress, DNA repair intermediates, and aborted enzymatic reactions (1,2). It is estimated that >10 000 SSBs form in each mammalian cell per day under normal conditions (3,4). SSBs can be repaired by a rapid global SSB repair mechanism or alternatively via homologue-mediated recombination or repair pathways (1,5). It is well documented that PARP1 and XRCC1 are implicated in the SSB repair pathway (6–9). Unrepaired SSBs compromise DNA replication and transcription, leading to genome instability, and have been implicated in cancer and neurodegenerative diseases (1,10–12). However, it remains unclear exactly how SSBs are sensed, signaled, and repaired in a coordinated fashion.

To preserve genome integrity, AP endonuclease 1 (APE1) plays essential roles in the repair of oxidative stress-induced DNA damage, such as AP sites (13–15). APE1 exhibits AP endonuclease, 3′–5′ exonuclease, 3′-phosphodiesterase as well as 3′ RNA phosphatase and 3′ exoribonuclease activities (16–18). APE1 is essential for early embryonic development in mice, and with the exception of a tissue-specific mouse B cell knockout line, APE1-null cells do not generally survive (19,20). In addition to its roles in redox-related transcriptional regulation, APE1 is critical for the base excision repair (BER) and nucleotide incision repair (NIR) pathways (14,21). Because some APE1 mutations result in deficiencies in both the endonuclease and exonuclease activities and some known APE1-specific inhibitors also inhibit both functions, it is technically challenging to separate the potential roles of these two activities of APE1 in maintaining genome integrity, especially in mammalian cells. Thus, it remains unclear whether APE1 plays direct roles in the repair and signaling of SSBs and what significance APE1's exonuclease activity plays in the maintenance of genome integrity.

The *Xenopus laevis* egg extract system including low-speed supernatant (LSS) and high-speed supernatant (HSS) offers a unique opportunity for mechanistic studies in the areas of DNA repair, the DNA damage response (DDR), and other genome integrity assurance pathways (22–24). Detailed approaches to prepare these LSS and HSS extracts have been described previously (25,26). In short, LSS and HSS are prepared from fractions of *Xenopus* eggs after centrifugation with different speed. Chromatin DNA can be added to LSS to recapitulate DNA replication in mammalian cells, and DNA damaging agents can damage DNA to trigger DNA repair and DDR pathways. Defined DNA structures such as plasmid with defined damage can be added to HSS for elucidating molecular details of DNA repair and signaling pathways (27).

We recently demonstrated that an ATR–Chk1-mediated DDR pathway is triggered via SSBs indirectly induced by oxidative stress in *Xenopus* LSS system and that AP en-

*To whom correspondence should be addressed. Tel: +1 704 687 8528; Fax: +1 704 687 1488; Email: shan.yan@uncc.edu
†The authors wish it to be known that, in their opinion, the first two authors should be regarded as Joint First Authors.

donuclease 2 (APE2) plays an essential role in this process (28,29). We have also revealed that a site-specific plasmid-based SSB structure triggers activation of an ATR–Chk1 DDR pathway in a APE2-dependent but replication-independent manner in the *Xenopus* HSS system (30). Recent data from budding yeast have revealed that APE2 is critical for 3′–5′ SSB end resection to suppress mutagenesis at sites of RNA misincorporation (31,32). Importantly, APE2 has been proposed as a synthetic lethal target of BRCA2 (33). Because APE2 is important for the continuation, but not the initiation, phase of 3′–5′ SSB end resection (30,34), it remains unclear how APE2 recruitment and its activity are regulated. In this work, we performed experiments with *Xenopus* egg extract and nuclear extract from cultured human cell line to provide evidence that APE1 is a critical upstream regulator of APE2 and that it plays essential and distinct roles in the repair and signaling of SSBs in eukaryotic systems.

MATERIALS AND METHODS

Experimental procedures for egg extracts and chromatin preparation, SSB signaling technology and plasmid DNA bound fraction isolation in *Xenopus laevis*

The Institutional Animal Care and Use Committee at University of North Carolina at Charlotte approved the care and use of *X. laevis*. Sperm chromatin was prepared and utilized according to methods described previously (25,26,28,35). The preparation of *Xenopus* LSS and HSS were described previously (25–27). Generally speaking, immunodepletion of target proteins in HSS and LSS was performed with a similar procedure as previously described (28–30,35). For APE1 depletion in HSS, 40 μl of HSS was incubated with ∼20 μl of ProteinA Sepharose beads (GE Healthcare) coupled with 20 μl of anti-APE1 antibodies for 30 min at 4°C. Typically, three-round depletion is needed to make ∼20 μl of APE1-depleted HSS from 40 μl of HSS.

The SSB signaling experiment setup and DNA-bound fractions from the HSS system have been described in more details recently (24,30). Typically, 48 μl of HSS was supplemented with 12 μl of either control or SSB plasmid (see below section for details) to a final concentration of 75 ng/μl. After different incubation times at room temperature, the 10 μl of reaction mixture (i.e. HSS–plasmid mixture) was added with sample buffer for immunoblotting analysis, and the remaining 50 μl of reaction mixture was diluted with 200 μl of egg lysis buffer (250 mM sucrose, 2.5 mM $MgCl_2$, 50 mM KCl, 10 mM HEPES, pH 7.7) for DNA-bound isolation and analysis via immunoblotting analysis.

Preparation of plasmids and FAM-, Cy5- or biotin-labeled DNA structures

The control (CTL) plasmid, SSB plasmid and DSB plasmid was described previously (24,30). Briefly, pUC19-derived plasmid pS (designated as CTL plasmid) contains only one recognition site of Nt.BstNBI. pS plasmid was catalyzed by Nt.BstNBI and CIP (calf intestine phosphatase) to make SSB plasmid, and by SbfI and CIP to make DSB plasmid. These plasmids were purified via QIAquick gel extraction kit and phenol–chloroform extraction.

The CTL2 plasmid in Supplementary Figure S3F was designated as pS2, which was derived from pcDNA3-YFP with a point mutation C3912A to create another NsiI recognition site. There is only one Nb.BsmI recognition site in the pS2 (i.e. T3913–C3919). To prepare the SSB2 plasmid with a site-specific SSB between the G3914 and C3915 on + strand in Supplementary Figure S3F, the pS2 was treated by Nb.BsmI and dephosphorylated by CIP followed by agarose gel purification and phenol–chloroform extraction. The SSB2 plasmid was verified by the generation of two fragments (i.e. ∼1300 and ∼4800 bp) after NsiI digestion, while one ∼6000 bp product was generated from the CTL2 plasmid after NsiI digestion. The pcDNA3-YFP was a gift from Doug Golenbock (Addgene plasmid # 13033; http://n2t.net/addgene:13033; RRID:Addgene_13033).

The 70bp FAM-labeled dsDNA structure was derived from the nt 406–475 fragment within the pS plasmid. Two complementary oligos (Forward Oligo #1: [FAM]-5′-TCGGTACCCGGGGATCCTCTAGAGTCGACC TGCAGGCATGCAAGCTTGGCGTAATCATGGTC ATAGCTGT-3′; Reverse Oligo #1: 5′- ACAGCTATGA CCATGATTACGCCAAGCTTGCATGCCTGCAGG TCGACTCTAGAGGATCCCCGGGTACCGA-3′) were annealed by incubation at 95–100°C for 5 min followed by natural cooling down at room temperature for ∼30 min to make the FAM-labeled dsDNA structure. The dsDNA structure was treated with Nt.BstNBI and CIP to make the dsDNA–SSB structure. The dsDNA–SSB structure was purified from agarose via QIAquick gel extraction kit and then phenol–chloroform extraction. To generate the dsDNA–gap structure, the dsDNA–SSB structure was treated with recombinant WT GST–APE1 in APE1 Reaction Buffer (50 mM HEPES pH 7.4, 60 mM NaCl, 2 mM $MgCl_2$ and 2 mM DTT) followed by phenol–chloroform extraction and purification using a similar procedure described previously (30,36). The FAM-labeled dsDNA–SSB–biotin structure in Supplementary Figure S5D was annealing of two complementary oligos (Forward Oligo #1: see above; Reverse Oligo #1.2: biotin–5′-ACAGCTAT GACCATGATTACGCCAAGCTTGCATGCCTGCA GGTCGACTCTAGAGGATCCCCGGGTACCGA-3′) followed by Nt.BstNBI and CIP treatment as well as gel and phenol–chloroform extraction.

The Cy5-SSB structure used in MST experiment in Figure 3E was annealing of two complementary oligos (Forward Oligo #1.2: Cy5-5′-TCGGTACCCGGGGA TCCTCTAGAGTCGACCTGCAGGCATGCAAGCT TGGCGTAATCATGGTCATAGCTGT-3′; and Reverse Oligo #1.2, see above) followed by Nt.BstNBI and CIP treatment as well as gel and phenol–chloroform extraction.

The biotin–dsDNA structure used in Supplementary Figure S6C was annealing two complementary strands with biotin labels in 5′-side (Forward Oligo #1.3: biotin–5′-TCGGTACCCGGGGATCCTCTAGAGTCGACCTG CAGGCATGCAAGCTTGGCGTAATCATGGTCAT AGCTGT-3′; Reverse Oligo #1.2, see above). The biotin–dsDNA structure was treated with Nt.BstNBI and CIP to make the biotin–dsDNA–SSB structure. The biotin–dsDNA–SSB structure was purified from agarose via QIAquick gel extraction kit and then phenol–chloroform extraction. To generate the biotin–dsDNA–gap structure,

the biotin–dsDNA–SSB structure was treated with recombinant WT GST-APE1 in APE1 Reaction Buffer followed by phenol–chloroform extraction.

The 39-bp FAM-labeled dsDNA-AP structure was prepared by annealing of two complementary oligos (Forward Oligo #2: [FAM]-5′- TGCTCGTCAAGAGTTCGTAA[THF]ATGCCTACACTGGAGATC-3′; Reverse Oligo #2: 5′-GATCTCCAGTGTAGGCATCTTACGAACTCTTGACGAGCA-3′). The dsDNA-AP structure was treated with DA GST–APE1 in APE1 Reaction Buffer followed by CIP treatment, gel and phenol–chloroform extraction to make the dsDNA–AP–SSB structure. The dsDNA–AP structure was treated with WT GST–APE1 in APE1 Reaction Buffer followed by CIP treatment, gel and phenol–chloroform extraction to make the dsDNA–AP–gap structure. WT GST–APE1 can cleave the dsDNA–AP structure and further resect it ∼1–3nt into gapped structures (Supplementary Figure S4B); in contrast, DA GST–APE1 only cleaves the dsDNA–AP structure without further end resection due to its exonuclease activity deficiency (Supplementary Figure S4D).

Cell culture and preparation of nuclear extract

U2OS cells were purchased from ATCC, and cultured in DMEM supplemented with 10% FBS. The nuclear extract were prepared following the below protocol. Cells were washed with phosphate-buffered saline (PBS) and resuspended in Solution A (20 mM Tris–HCl pH 7.4, 10 mM NaCl, 3 mM $MgCl_2$). After a 15-min incubation on ice, Nonidet P-40 was added to a final concentration of 0.5% and vortex for 10 s at highest setting. Then the samples were spun at low speed (3000 rpm for 10 min) to separate cytoplasmic fraction and permeabilize nuclei. These nuclei were recovered and lysed with Solution B (20 mM Tris–HCl pH 8.0, 150 mM NaCl, 2 mM EDTA, 0.5% Nonidet P-40, 0.5 mM Na_3VO_4, 5 mM NaF, 5 μg/ml of Aprotinin and 10 μg/ml of Leupeptin). The nuclear extracts were isolated by centrifugation at 13 000 rpm for 30 min.

Recombinant DNA and proteins

Recombinant pGEX-4T1-APE1 was prepared by PCR full length (corresponding to the nt 119–1069) *Xenopus* APE1(GenBank ID: BC072056; MGC:78928) with two primers (Forward Oligo #3: 5′-GGGGGGGATCCATGCCCAAGAGAGGGAAGAAG-3′; Reverse Oligo #3: 5′-GGGGGCTCGAGTTATATGGCCATCAAGAGTG-3′) and subcloned into pGEX-4T1 at BamHI and XhoI sites. The nucleotide sequences of deletion mutants GST-APE1 are as follows AA 35–316, nt 221–1069; AA 101–316, nt 419–1069; AA 101–200, nt 419–718; AA 201–316, nt 719–1069. Recombinant pCS2+MT-APE1 was prepared by PCR *Xenopus* APE1 with two primers (Forward Oligo #3.2: 5′-GGGGGCCATGGAGATGCCCAAGAGAGGGAAGAAG-3′; Reverse Oligo #3) and subcloned into pCS2 + MT at NcoI and XhoI sites. QuikChange II XL Site-Directed Mutagenesis kit (Agilent) was utilized to generate various point mutant recombinant plasmids. Recombinant plasmids were prepared via QIAprep spin miniprep kit following vendor's standard protocol.

pGEX-4T1-APE2, pGEX-4T1-APE2-ZF, pGEX-4T1-APE2-ZF-C470A, pGEX-4T1-APE2-ZF-R502E, pCS2+MT-APE2, pCS2+MT-APE2-ΔZF have been described previously (28–30). GST- or His-tagged recombinant proteins were expressed and purified in *Escherichia coli* DE3/BL21 following vendor's standard manual. Purified recombinant proteins were examined on SDS-PAGE gels with coomassie staining. Myc-tagged recombinant proteins were generated TNT SP6 Quick Coupled Transcription/ Translation System (Promega) with recombinant pCS2+MT-derived plasmids according to vendor's protocol.

Immunoblotting analysis and antibodies

Anti-*Xenopus* APE1 antibodies were raised in rabbits against purified GST–APE1 (Cocalico Biologicals). Anti-*Xenopus* APE2 antibodies were described previously (28). Antibodies against ATR, ATRIP, Rad9, Rad17, TopBP1 and RPA32 were kindly provided by Drs Karlene Cimprich, Howard Lindsay, and Matthew Michael (35,37,38). Antibodies against RPA32 phosphorylation at Ser33 (Bethyl Laboratories, Cat# A300-246A), Chk1 phosphorylation at Ser345 (Cell Signaling Technology, Cat# 2348), Histone 3 (Abcam, Cat# ab1791), Chk1 (Santa Cruz Biotechnology, Cat# sc-7898), GST (Santa Cruz Biotechnology, Cat# sc-138), His (Santa Cruz Biotechnology, Cat# sc-8036), Myc (Santa Cruz Biotechnology, Cat# sc-40), PCNA (Santa Cruz Biotechnology, Cat# sc-56), and Tubulin (Santa Cruz Biotechnology, Cat# sc-8035) were purchased from various commercially available vendors. Antibodies against human RPA32 (Thermo Fisher Scientific, Cat# MA126418) and Chk1 (Cell Signaling Technology, Cat# 2360) were purchased from available vendors. Immunoblotting analysis was performed following procedures described previously (28,30,35).

GST pulldown assays

For the GST-pulldown experiments, 5 μg of GST or GST-tagged recombinant proteins, and 5 μg of either WT or mutant His-tagged PCNA, or 20 μl of TNT SP6 reactions containing various Myc-tagged recombinant proteins were added to 200 μl of Interaction Buffer (100 mM NaCl, 5 mM $MgCl_2$, 10% (vol/vol) glycerol, 0.1% Nonidet P-40, 20 mM Tris–HCl at pH 8.0). After an hour of incubation, an aliquot of the mixture was collected as Input and the remaining mixture was supplemented with 100 μl of Interaction Buffer that contains 30 μl of glutathione beads. After incubation with rotation for 1 h at room temperature or overnight at 4°C, bead-bound fractions were washed twice with Interaction Buffer. Then, the input and bead-bound fractions were examined via immunoblotting analysis as indicated.

Analysis of DNA repair products from the HSS system

The procedures of isolating DNA repair products of SSB plasmid from the HSS system have been described with more details recently (24,30). Briefly, after incubation of SSB plasmid in the HSS, the reactions were resuspended in nuclease-free water, extracted with phenol–chloroform, and

precipitated by ethanol with the presence of sodium acetate and glycogen. The resuspended and purified DNA repair products were examined on agarose gel and stained with ethidium bromide.

SSB end resection assays in the HSS system

As experiment design shows, various FAM-labeled DNA structures were added to mock- or depleted HSS, which was supplemented with WT/mutant Myc-tagged recombinant proteins as indicated, respectively. After different times of incubation at room temperature, reactions were quenched with equal volume of TBE–urea Sample Buffer (Invitrogen), denatured at 95°C for 5 min. Samples were examined on 18% TBE–urea gel and imaged on Typhoon 8600 and viewed using ImageQuant software.

In vitro endo/exonuclease assays

For *in vitro* endonuclease assays, the dsDNA–AP structure was treated with different concentrations of purified recombinant proteins such as WT or mutant GST–APE1 in APE1 Reaction Buffer. At indicated time intervals, 10 μl of endonuclease assay reaction was quenched with the addition of 10 μl of TBE–urea Sample Buffer and immediately denatured at 95°C for 5 min. For *in vitro* exonuclease assays, the dsDNA–SSB structure was treated with different concentrations of purified recombinant proteins such as WT or mutant GST–APE1 in APE1 Reaction Buffer at 37°C. After different times of incubation, exonuclease assay reactions were quenched with equal volume of TBE–urea Sample Buffer and denatured at 95°C for 5 min. After a quick 10-second spin, still-hot samples were resolved on 18% TBE–urea PAGE gel. Gels were imaged with a Typhoon 8600 imager (GE Healthcare) and analyzed using ImageJ.

Electrophoretic mobility shift assays (EMSA)

For EMSA assays, different concentrations of purified recombinant proteins were incubated with 10 nM of various FAM-labeled DNA structures in EMSA Reaction Buffer (10 mM Tris pH 8.0, 50 mM NaCl, 0.2 mM TCEP, 5% glycerol) at a final volume of 10 μl for 3 h at 4°C. Reactions were resolved on a 4–20% TBE native gel at 4°C and imaged using a Typhoon 8600 imager (GE Healthcare).

Microscale thermophoresis (MST) assays

First, 50 nM of the substrate (i.e. Cy5–SSB substrate, see Figure 3E) was mixed with different concentrations (15 times of 1:2 v/v series of dilutions with 25 μM as starting concentration) of ligand protein (GST, GST-WT APE1 or GST-DA APE1) in the Buffer A (80 mM NaCl, 20 mM β-glycerophosphate, 2.5 mM EGTA, 0.01% NP-40 and 10 mM HEPES–KOH, pH 7.5). The mixtures were incubated at room temperature for 15 min, followed by filling into individual capillaries, respectively. Based on the absorption and emission wavelength of the Cy5 (646/662 nm), 'Red' mode of the Monolith NT.115 was chosen for the MST test.

DNA binding assays

For the biotin–dsDNA binding assays in Supplementary Figure S6C, the biotin–dsDNA, biotin–dsDNA–SSB or biotin–dsDNA–gap structure was coupled to Streptavidin Dynabeads using the approach previously described (30). Then beads were mixed with Myc-APE1 in Buffer B (80 mM NaCl, 20 mM β-glycerophosphate, 2.5 mM EGTA, 0.01% NP-40, 10 mM $MgCl_2$, 100 μg/ml BSA, 10 mM DTT and 10 mM HEPES–KOH, pH 7.5). After incubation at 4°C for 30 min, aliquots of mixture were collected as Input, and the beads were washed with Buffer A for three times. The input and bead-bound fractions were analyzed via immunoblotting analysis.

RESULTS

APE1 is required for APE2 regulation and activation of SSB-induced ATR–Chk1 DDR pathway

The APE1 protein contains an N-terminal nuclear localization domain (NLS), a middle Redox domain, and a C-terminal endonuclease/exonuclease/phosphatase (EEP) domain (Supplementary Figure S1A). The APE1 amino acid sequence is highly conserved across frog, mouse and human; and *X. laevis* APE1 and human APE1 share 66% identity and 77% similarity (Supplementary Figure S1B), suggesting that APE1 has evolutionarily conserved roles. To investigate the role of APE1 in genome integrity, we first expressed and purified recombinant *Xenopus* wild type (WT) GST–APE1 protein (Supplementary Figure S2A). The purified WT GST–APE1 recombinant protein was used to make custom anti-APE1 antibodies. Our custom anti-APE1 antibody, but not prebleed, can recognize endogenous APE1 in *Xenopus* LSS and HSS, as well as recombinant GST–APE1 and Myc-APE1 protein, but not control TNT reaction without expression plasmid (Supplementary Figure S2B and C). The custom anti-APE1 antibody can be used to effectively deplete APE1 from *Xenopus* HSS (Figure 1A, Supplementary Figure S3A). Our recent study showed that a defined SSB plasmid activates the ATR–Chk1 DDR pathway in *Xenopus* HSS (30). Notably, the SSB-induced Chk1 phosphorylation was absent in APE1-depleted HSS (Figure 1A, Supplementary Figure S3A), suggesting that APE1 plays an important role in the SSB-induced ATR–Chk1 DDR pathway.

Several small-molecule APE1-specific inhibitors have been identified that target its AP endonuclease activity (e.g. AR03, APE1 inhibitor III (APE1i III) and CRT0044876) or its redox regulatory activity (e.g. E3330) (39–42). Importantly, we found that AR03 and APE1i III compromised the SSB-induced Chk1 phosphorylation in the HSS system (Figure 1B). We also found that the impairment of SSB-induced Chk1 phosphorylation by AR03 treatment was dose-dependent (Supplementary Figure S3B). Notably, the compromised SSB-induced Chk1 phosphorylation by AR03 was rescued by the addition of WT, but not DA, GST–APE1 protein in the HSS system (Supplementary Figure S3C). Furthermore, we found that APE1i III and AR03 inhibited both the endonuclease and exonuclease activities of recombinant *Xenopus* APE1 *in vitro*, whereas CRT0044876 and E3330 had minimal effects on these activ-

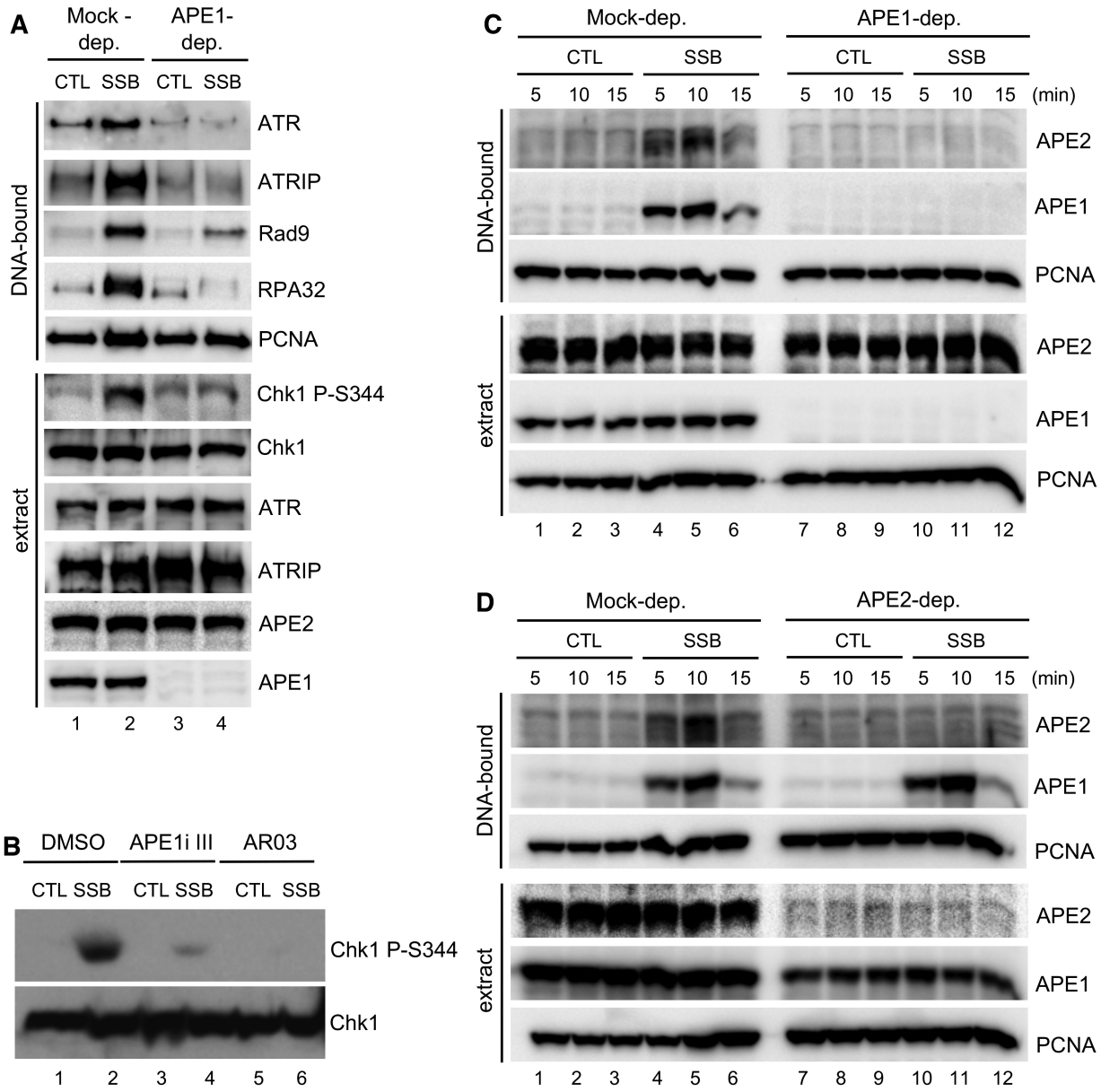

Figure 1. APE1 is required for SSB-induced ATR–Chk1 DDR pathway activation and APE2 recruitment to SSB sites, but not *vice versa.* (**A**) CTL or SSB plasmid was added to mock- or APE1-depleted HSS. After incubation for 30 min, the DNA-bound fractions and total egg extract were examined via immunoblotting analysis as indicated. (**B**) CTL or SSB plasmid was added to HSS supplemented with APE1i III or AR03 at a final concentration of 1 mM. (**C–D**) CTL or SSB plasmid was added to mock-, APE1- or APE2-depleted HSS. The DNA-bound fractions and total egg extract at the indicated timepoints were examined via immunoblotting analysis.

ities (Supplementary Figure S4A–C). Because APE1's endonuclease activity is dispensable for the generation of the break in our plasmid-based experimental system, our observations suggest that APE1's exonuclease activity is important for SSB-induced DDR pathway activation in the HSS system.

We recently demonstrated that hydrogen peroxide-derived SSBs from chromatin DNA trigger the activation of ATR–Chk1 DDR pathway in *Xenopus* LSS system (28,29). We confirmed that the hydrogen peroxide-induced Chk1 phosphorylation was absent in APE1-depleted LSS (Supplementary Figure S3D). Furthermore, addition of APE1i III or AR03 compromised the hydrogen peroxide-induced Chk1 phosphorylation in the LSS system (Supplementary Figure S3E). These results in the *Xenopus* LSS system suggest that APE1 is important for activation of the ATR–Chk1 DDR pathway by SSBs indirectly generated on chromatin DNA by hydrogen peroxide treatment.

To test whether the critical role of APE1 in SSB-induced ATR activation is conserved in humans, we prepared nuclear extract from cultured human bone osteosarcoma U2OS cells and found that another plasmid carrying a defined SSB site (designed as SSB2), but not the control plasmid (CTL2), triggered Chk1 phosphorylation and RPA32

phosphorylation in U2OS nuclear extract (Supplementary Figure S3F). Notably, addition of APE1i III or AR03 compromised the Chk1 phosphorylation and RPA32 phosphorylation induced by the defined SSB2 plasmid (Supplementary Figure S3F). These observations suggest that APE1's exonuclease activity is critical for its function in SSB-induced ATR DDR pathway in humans, representing a conserved function of APE1 during evolution.

To dissect the underlying mechanism of APE1's role in SSB-induced DDR activation, we isolated the DNA-bound fractions from the HSS and examined the abundance of checkpoint proteins via immunoblotting analysis. Notably, the recruitment of RPA32 to the SSB plasmid was compromised when APE1 was depleted from the HSS ('DNA-bound', Figure 1A), suggesting that APE1 contributes to ssDNA generation at the SSB site. Furthermore, the assembly of a checkpoint protein complex that includes ATR, ATRIP, and Rad9 on the SSB plasmid (but not on the CTL plasmid) was compromised in APE1-depleted HSS (Figure 1A). The phenotype caused by APE1-depletion is very similar to that caused by APE2-depletion (30); however, it is intriguing that the presence of APE2 cannot compensate for APE1 depletion (Figure 1A). We reason that APE1 may play an indispensable upstream role for APE2's function in SSB signaling. In our analysis of the dependency between APE1 and APE2 in SSB signaling, we found that APE2 recruitment to the SSB plasmid (but not to the CTL plasmid) was significantly compromised in APE1-depleted HSS ('DNA-bound', Figure 1C). However, APE2 depletion had no effects on APE1 recruitment to the SSB plasmid or to the CTL plasmid ('DNA-bound', Figure 1D). These observations provide direct evidence that APE1 plays a role upstream of APE2 in the SSB-induced ATR–Chk1 DDR pathway but not *vice versa* in *Xenopus* HSS system.

APE1 exonuclease activity is required for SSB signaling

To further determine the importance of APE1's exonuclease activity in SSB-induced DDR pathway activation, we sought to identify exonuclease-deficient but endonuclease-proficient APE1 variants from among several *Xenopus* APE1 mutants (Supplementary Figure S1). It has been demonstrated via *in vitro* exonuclease assays that human APE1 binds to a nick structure and removes 1–3 nucleotides (nt) in the 3′–5′ direction (36), and that the human APE1 D308A variant in the catalytic EEP region (corresponding to *Xenopus* APE1 D306A, designated as DA APE1, Figure 2C) lacks 3′–5′ exonuclease activity but retains its AP endonuclease activity (43,44). It was reported that a human APE1 variant carrying E96Q and D210N mutations in the catalytic EEP region (corresponding to *Xenopus* APE1 E95Q-D209N, designated as ED APE1, Supplementary Figure S1) is endonuclease-dead; however, it remains unclear whether an APE1 variant carrying C93A and C99A mutations in the redox region (corresponding to *Xenopus* APE1 C92A–C98A, designated as CA APE1, Supplementary Figure S1) is nuclease-proficient (45,46). Whereas WT APE1 had exonuclease activity indicated by the results of an assay with a FAM-labeled dsDNA with a defined SSB (designed as dsDNA–SSB), the ED, DA, and CA APE1 mutants lacked exonuclease activity under the conditions we tested (Figure 2A, Supplementary Figure S4D and E). Furthermore, WT, DA and CA APE1, but not ED APE1, were proficient for endonuclease activity in an assay with a defined AP-mimicking tetrahydrofuran (THF)-containing substrate (designed as dsDNA–AP) under the conditions we tested (Figure 2B). Control experiment shows that no noticeable change was observed for the binding of WT, DA or CA APE1 to the dsDNA–AP structure in EMSA assays (Supplementary Figure S5A). Therefore, DA and CA APE1 are proficient for endonuclease activity but deficient in exonuclease activity. Of note, the D306, C92 and C98 residues in *Xenopus* APE1 share identity with human and mouse APE1 (Figure 2C, Supplementary Figure S1B).

To characterize the biological significance of APE1's exonuclease activity, we added back WT or DA Myc-tagged APE1 to APE1-depleted HSS and found that WT APE1, but not DA APE1, rescued SSB-induced Chk1 phosphorylation (Figure 2D). This observation suggests that APE1's exonuclease activity is important for activation of the SSB-induced ATR–Chk1 DDR pathway in the HSS system. Importantly, WT APE1, but not DA APE1, rescued the recruitment of RPA32, ATR, ATRIP, TopBP1 and Rad9 to the SSB plasmid in APE1-depleted HSS (Figure 2D). Of note, APE2 was recruited to the SSB plasmid when WT APE1 but not DA APE1 was added back to APE1-depleted HSS even though WT and DA APE1 were similarly recruited to the SSB plasmid (Figure 2E). These observations indicate that APE1's exonuclease activity is important for APE2 recruitment to the SSB site. Taken together, our data demonstrate that APE1's exonuclease activity is critical for APE2 recruitment and checkpoint protein complex assembly onto SSB sites as well as for SSB-induced ATR–Chk1 DDR pathway activation.

APE1 recognizes and binds to SSB structures *in vitro*

Our observations so far suggest that SSBs may first be sensed and recognized by APE1. To address this question directly, we tested whether APE1 preferentially interacts with SSB sites to generate a 1–3nt gap that in turn leads to APE1 dissociation or reduced interaction. We prepared several defined FAM-labeled DNA structures, including the dsDNA–SSB, the dsDNA–AP, dsDNA with an AP-site-derived SSB (designed as dsDNA–AP–SSB), as well as gapped structures derived from dsDNA–SSB or dsDNA–AP–SSB (designated as dsDNA–gap or dsDNA–AP–gap). Upon addition of higher concentrations of purified recombinant WT GST–APE1 (∼20–40 μM), significant mobility shifts of the dsDNA–SSB structure were detected in an EMSA assay, suggesting that APE1 interacts with SSBs to form DNA–protein complexes (Figure 3A). However, there were almost no mobility shifts of the dsDNA and dsDNA–gap structures with similar concentrations of WT GST–APE1 protein (Figure 3A). These results indicate that APE1 preferentially interacts with the defined SSB structure over the dsDNA or dsDNA–gap structures. Furthermore, we found that WT GST–APE1 protein preferentially interacted with the dsDNA–AP–SSB structure, which mimics the SSB structure derived from an AP site (Figure 3B). The binding of WT GST–APE1 to the dsDNA–AP and dsDNA–AP–gap structures was decreased to some extent in compari-

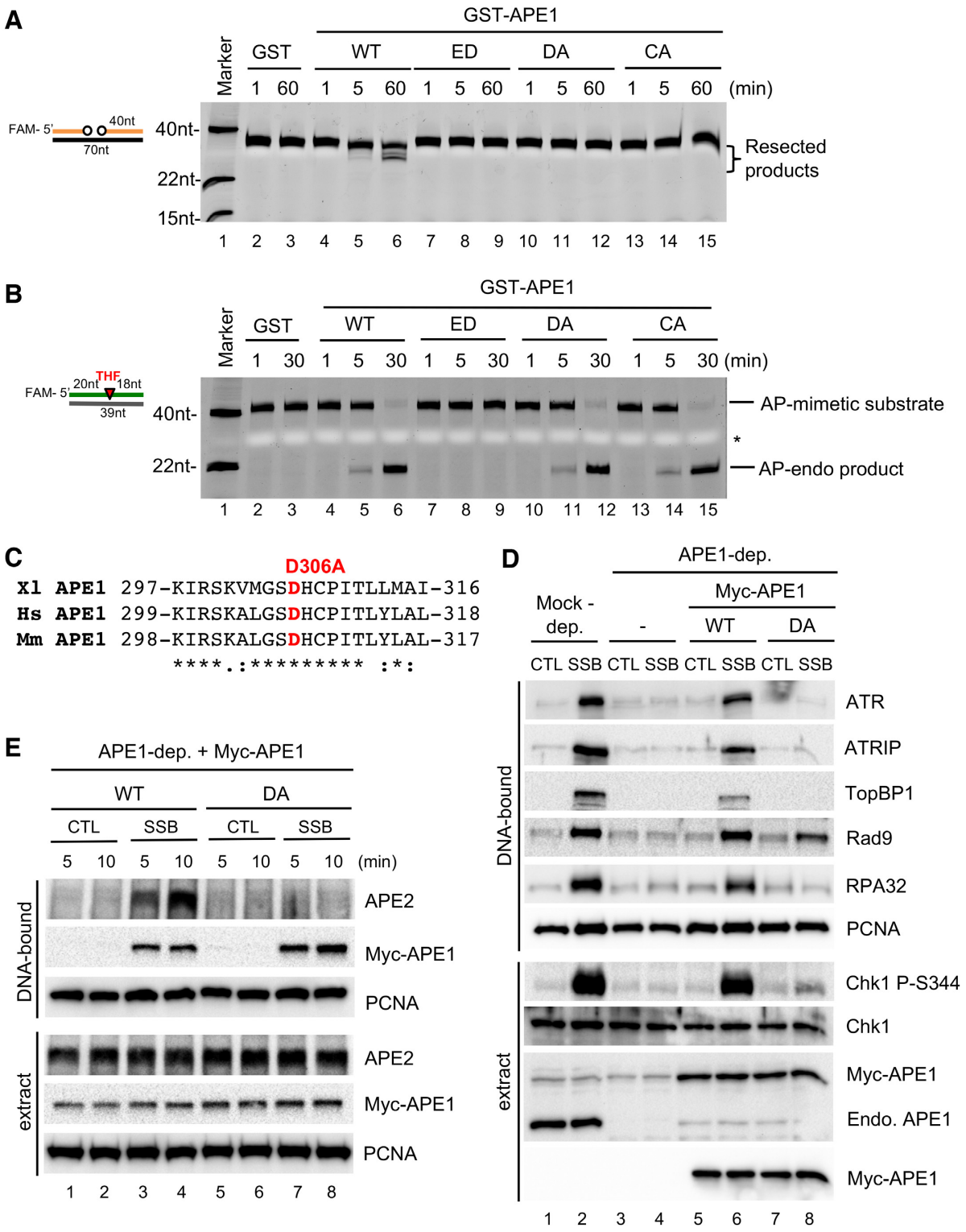

Figure 2. APE1 exonuclease activity is important for APE2 recruitment to SSB sites and ATR–Chk1 DDR pathway activation. (**A**) Characterization of the exonuclease activities of WT and mutant GST–APE1 (4 μM) after different incubation times in *in vitro* exonuclease activity assays. WT, wild type; ED, E95Q–D209N; DA, D306A; CA, C92A–C98A. (**B**) Characterization of the endonuclease activities of WT and mutant GST–APE1 (0.08 μM) via *in vitro* endonuclease activity assays. * nonspecific dye band from sample buffer. (**C**) An amino acid alignment highlights the conserved D306 residue in *Xenopus*, humans, and mouse APE1. (**D**) WT or DA Myc-APE1 was added back to APE1-depleted HSS supplemented with CTL or SSB plasmid. After incubation for 30 min, the DNA-bound fractions and total egg extract were examined via immunoblotting. (**E**) CTL or SSB plasmid was added to APE1-depleted HSS that was mixed with WT or DA Myc-APE1. After different incubation times (5 and 10 min), the DNA-bound fractions and total egg extract were examined via immunoblotting.

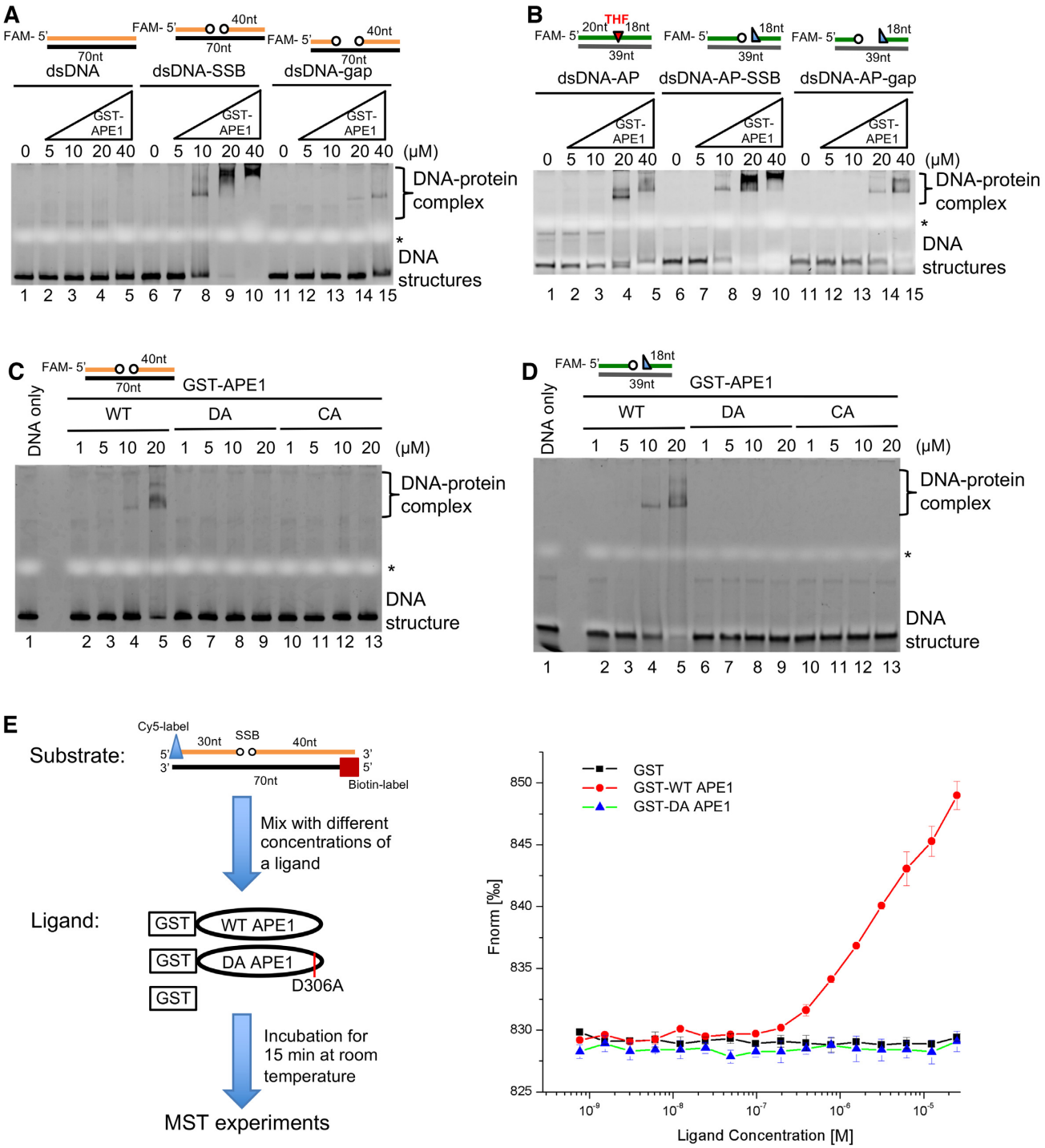

Figure 3. APE1 recognizes and binds to SSB structures *in vitro*. (**A**) EMSAs show the interactions between GST–APE1 and various DNA structures: dsDNA, dsDNA–SSB and dsDNA–gap. (**B**) Interactions between GST–APE1 and various DNA structures: dsDNA–AP, dsDNA–AP–SSB and dsDNA–AP–gap. (**C**) An EMSA showing the interaction between WT, DA and CA GST–APE1 and the dsDNA–SSB structure. (**D**) Interactions between WT, DA, and CA GST–APE1 and the dsDNA–AP–SSB structure via an EMSA. *nonspecific dye band from sample buffer in panels (A–D). (**E**) Interactions of GST-tagged WT and DA APE1 as well as GST to the defined Cy5–SSB structure via MST (Microscale Thermophoresis) assays.

son to its binding to the dsDNA–AP–SSB structure (Figure 3B). Control EMSAs demonstrated that GST alone did not interact with any of the DNA structures (Supplementary Figure S5B and C). In addition, neither DA APE1 nor CA APE1 formed complexes with the dsDNA–SSB or dsDNA–AP–SSB structure (Figure 3C and D), suggesting that direct interaction between APE1 and SSB structure is important for APE1's exonuclease activity *in vitro*.

In addition to the EMSA assays, Microscale Thermophoresis (MST) approach was utilized to quantify the binding of GST-tagged WT or DA APE1, or GST, to a Cy5-labeled SSB substrate (designated as Cy5–SSB), which contains a defined SSB in the middle, a Cy5 in the N-terminus and a biotin in the C-terminus (Figure 3E). The Cy5 and biotin labels on the termini of Cy5–SSB likely prevent recognition and binding of its ligand protein to its DSB ends. The MST analysis suggests that GST-WT APE1, but not GST-DA APE1 nor GST, can bind to the defined Cy5–SSB structure (Figure 3E). We repeated this experiment three times, and found that the K_d of WT APE1 interaction with the defined Cy5–SSB structure was 2.89 ± 0.10 μM. Taken together, our evidence using EMSA and MST assays indicates that APE1 recognizes and preferentially binds to SSB structures *in vitro*.

APE1 is required for SSB end resection and SSB repair in the HSS system

Next, we test whether APE1 is important for the end resection of several defined FAM-labeled DNA structures the *Xenopus* HSS system. First, the 30-nt FAM-labeled ssDNA within the dsDNA–SSB structure will be getting shorter and shorter if such SSB structure is resected in the 3′–5′ direction in the HSS system. After different incubation times in the HSS, the dsDNA–SSB structure was resected into Type I resection products in the 3′–5′ direction in the HSS (Figure 4A), consistent with our recent studies (30). After 5- and 30-minute incubations in the HSS system, some repaired products of the dsDNA–SSB (labeled as 'Repaired products') appeared at the expected size ∼70 nt assuming that the resected gap is filled and ligated (i.e., ∼30 nt + 40 nt) (lanes 3 and 4, Figure 4A). Importantly, the 3′–5′ end resection and repair of the dsDNA–SSB construct were almost entirely absent in APE1-depleted HSS (Figure 4A, Supplementary Figure S6A). Notably, addition of WT APE1, but not DA APE1, rescued the impaired SSB end resection and SSB repair in APE1-depleted HSS (compare lanes 10 and 13 with lane 7, Figure 4A). These observations suggest that APE1's exonuclease activity is important for end resection and repair of the defined dsDNA–SSB structure in the HSS system.

Second, we examined the role of APE1 in the end resection of the dsDNA–AP–SSB structure, which contains a 3′-OH and 5′-deoxyribose phosphate derived from the AP-mimetic dsDNA–AP structure. This substrate more mimics SSBs that are intermediate products during the DNA repair of AP sites. On denature urea gel, the dsDNA–AP–SSB structure appeared at ∼20-nt size, as expected (lanes 1 and 2, Figure 4B), and was resected into shorter Type I resection products (lanes 3 and 4, Figure 4B). Repaired products of the dsDNA–AP–SSB structure were observed

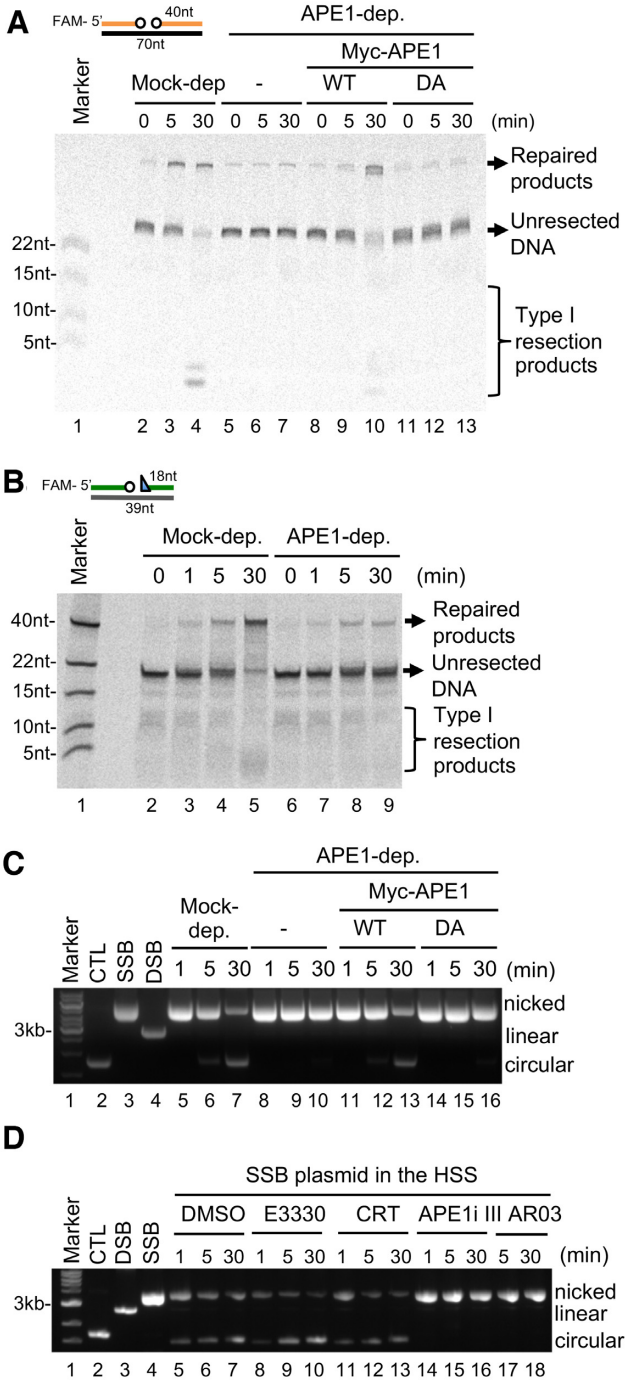

Figure 4. APE1 is critical for SSB end resection and SSB repair in the HSS system. (**A**) The dsDNA–SSB structure was added to mock- or APE1-depleted HSS supplemented with WT or DA Myc-APE1. After different incubation times, samples were examined via denaturing urea PAGE electrophoresis and visualized. (**B**) The dsDNA–AP–SSB structure was added to mock- or APE1-depleted HSS, and samples were analyzed the same as in Panel (**A**). (**C**) The SSB plasmid was added to mock- or APE1-depleted HSS supplemented with WT or DA Myc-APE1. After different incubation times, the DNA repair products were isolated and analyzed on an agarose gel. (**D**) The SSB plasmid was added to HSS supplemented with the different APE1-specific inhibitors (E3330, CRT0044876 (CRT), APE1i III and AR03) at a final concentration of 1 mM. After different incubation times, the DNA repair products were isolated and analyzed on an agarose gel.

at the expected size (∼39-nt) after 5-min and 30-min incubation in the HSS (lanes 3 and 4, Figure 4B). Consistent to the observations of the dsDNA–SSB structure in Figure 4A, we found that the end resection and repair of the dsDNA–AP–SSB structure were compromised in APE1-depleted HSS (Figure 4B). Importantly, the presence of APE2 in the APE1-depleted HSS could not compensate for the deficiency in SSB end resection of the two defined SSB structures (Figure 4A and B), further supporting APE1's role upstream of APE2. Taken together, our observations using these two defined SSB structures in the HSS system suggest that APE1 is essential for the initiation step in 3′–5′ SSB end resection.

Furthermore, we tested the role of APE1 in the repair of a THF-modified AP-mimicking structure (i.e., dsDNA-AP) in the HSS system. After incubation in the HSS system, the dsDNA–AP structure (indicated as ∼39-nt 'AP-mimetic substrate') was catalyzed into an intermediate SSB structure (indicated as ∼20-nt 'APE1-endo product') that was then further resected into Type I resection products (∼3-nt to 10-nt) (lanes 2–5, Supplementary Figure S6B). Notably, APE1 depletion in the HSS resulted in defective SSB generation from the dsDNA–AP structure (lanes 6–9, Supplementary Figure S6B), consistent with the notion that APE1 is the main AP endonuclease. Consistent with our recent report (30), the Type I resection products were compromised in APE2-depleted HSS (lanes 10–13, Supplementary Figure S6B).

After establishing the requirement of APE1 for SSB end resection in the HSS system, we intended to test a direct role of APE1 in SSB repair. After incubation in HSS, SSB plasmid was converted from a nicked version into a circular version ('nicked' versus 'circular' in lanes 5–7, Figure 4C), suggesting that SSB is repaired in HSS. We found that the repair of the SSB plasmid was compromised in APE1-depleted HSS, suggesting that APE1 is important for SSB repair (compare lanes 5–7 and lanes 8–10, Figure 4C). Of note, WT APE1, but not DA APE1, rescued the SSB repair deficiency in APE1-depleted HSS (compare lanes 11–13 and lanes 14–16, Figure 4C). Our evidence demonstrates a direct requirement for APE1's exonuclease activity in SSB repair. Furthermore, addition of APE1i III or AR03 compromised the repair of the SSB plasmid in the HSS system; in contrast, addition of E3330 or CRT0044876 had almost no noticeable effects on the repair of the SSB plasmid (Figure 4D). Collectively, these results indicate that APE1 and its exonuclease activity in particular are required for SSB repair.

APE1 interacts with APE2 and PCNA

Our data so far suggest that APE1 plays an essential role in the initiation stage of SSB end resection for SSB repair and SSB signaling. APE2 exhibits robust exonuclease activity but slower AP endonuclease activity under the tested conditions (30,34,47,48). While APE2 is recruited to SSB sites via its PIP box-mediated interaction with PCNA, APE2's exonuclease activity is fine-tuned by three distinct regulatory mechanisms, including APE2's Zf-GRF motif-mediated interaction with ssDNA and two modes of APE2–PCNA interaction (28–30,47). However, APE2 plays an important role in the continuation but not the initiation stage of SSB end resection (30). The next question is how SSB end resection is switched from APE1 to APE2 in HSS system.

First, we tested the possibility that APE1 may interact with APE2 by reciprocal protein–protein interaction assays. We observed that APE1 did indeed directly interact with APE2 *in vitro* (Figure 5A and B). Domain dissection experiments revealed that the first 100 amino acids of APE1 were dispensable for its interaction with APE2 (Figure 5C), and that multiple interaction sites within the catalytic domain of APE1 might mediate the APE2 interaction (Figure 5D). Similar to WT GST-APE1, DA GST-APE1 also interacted with Myc-APE2 *in vitro* (Figure 5B). On the other hand, the interaction with GST-APE1 was compromised when the Zf-GRF motif is depleted in Myc-APE2 in *in vitro* GST pulldown assays, suggesting that APE2's Zf-GRF motif is important for APE1 interaction (Figure 5E). Furthermore, GST-APE2-Zf-GRF but not GST interacted with Myc-APE1, suggesting a direct interaction between APE1 and APE2's Zf-GRF (Figure 5F). Although the R502 and C470 residues within the APE2 Zf-GRF motif are critical for its interaction with ssDNA and PCNA (29,30), WT, C470A and R502E GST-APE2 Zf-GRF remained the similar capacity to interact with Myc-APE1, suggesting that APE1 interaction is another distinct feature of the APE2 Zf-GRF motif (Figure 5F). It remains unclear whether the APE1–APE2 interaction plays a direct role in APE2 recruitment to SSB sites.

Because prior studies have shown that PCNA interacts with APE2 for its recruitment and activation (28,30,47,49), we intended to determine the potential role of PCNA in APE1's function in SSB repair and signaling. We found that WT, DA and CA GST-APE1 similarly interacted with His-tagged PCNA *in vitro* (Supplementary Figure S7A). Similar to WT PCNA, the mutant LI PCNA (L126A–I128A) interacted with GST-APE1 *in vitro* (Supplementary Figure S7B), although LI PCNA containing mutations in its interdomain connector loop (IDCL) does not interact with the PIP boxes of its interacting partners (30). These data suggest that APE1 interacts with PCNA directly *in vitro* through a non-canonical PIP box-mediated mechanism. Notably, the addition of PCNA protein had almost no noticeable effects on WT APE1's exonuclease activity (Supplementary Figure S7C). Taken together, these observations suggest that PCNA is dispensable for APE1's exonuclease activity under the conditions we tested, although PCNA interacts with APE1 and APE2 via different mechanisms.

Patient-derived APE1 mutants are deficient for SSB repair and signaling

Lastly, we aimed to test whether patient-derived APE1 variants are defective for SSB repair and SSB signaling. A CBioPortal query of data from 75,020 cancer patients in 256 studies revealed ∼99 different types of somatic alterations in human APE1, including missense mutations, truncations, and deletions (Figure 6A) (www.cbioportal.org). In particular, F266L and F266Y mutations in APE1 were present in a glioblastoma patient (Sample ID: TCGA-28-2506). Previous studies showed that the 3′–5′ exonuclease activity of human APE1 F266C and F266A mutants are enhanced

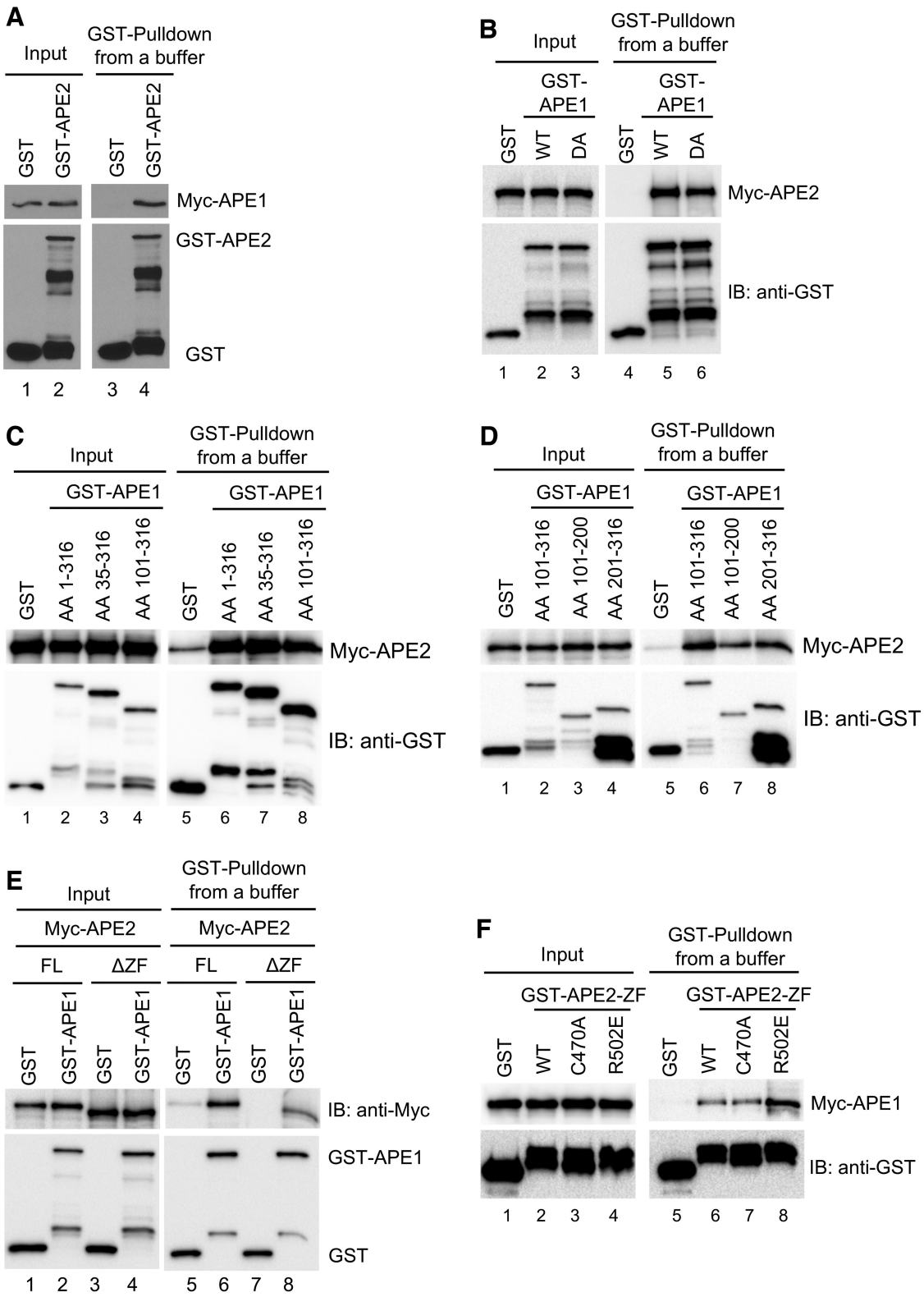

Figure 5. APE1 interacts with APE2. (**A**) GST or GST-APE2 was examined for interaction with Myc-APE1 in an interaction buffer. (**B**) GST, WT or DA GST-APE1 was examined for interaction with Myc-APE2 in an interaction buffer. (**C**) GST or GST-tagged different fragments (i.e. AA 1–316, AA 35–316 and AA 101–316) of APE1 was examined for interaction with Myc-APE2 in an interaction buffer. (**D**) GST or GST-tagged different fragments (i.e. AA 101–316, AA 101–200 and AA 201–316) of APE1 was examined for interaction with Myc-APE2 in an interaction buffer. (**E**) GST or GST-APE1 was examined for interaction with FL Myc-APE2 or ΔZF Myc-APE2 (i.e. Zf-GRF motif deletion mutant in APE2) in an interaction buffer. (**F**) GST, and WT/C470A/R502E GST-APE2-ZF were analyzed for interaction with Myc-APE1 in an interaction buffer. WT GST-APE2-ZF is GST-tagged Zf-GRF motif of APE2 (i.e. AA 456–517 in APE2). (A–F) Input and pulldown samples were analyzed via immunoblotting analysis.

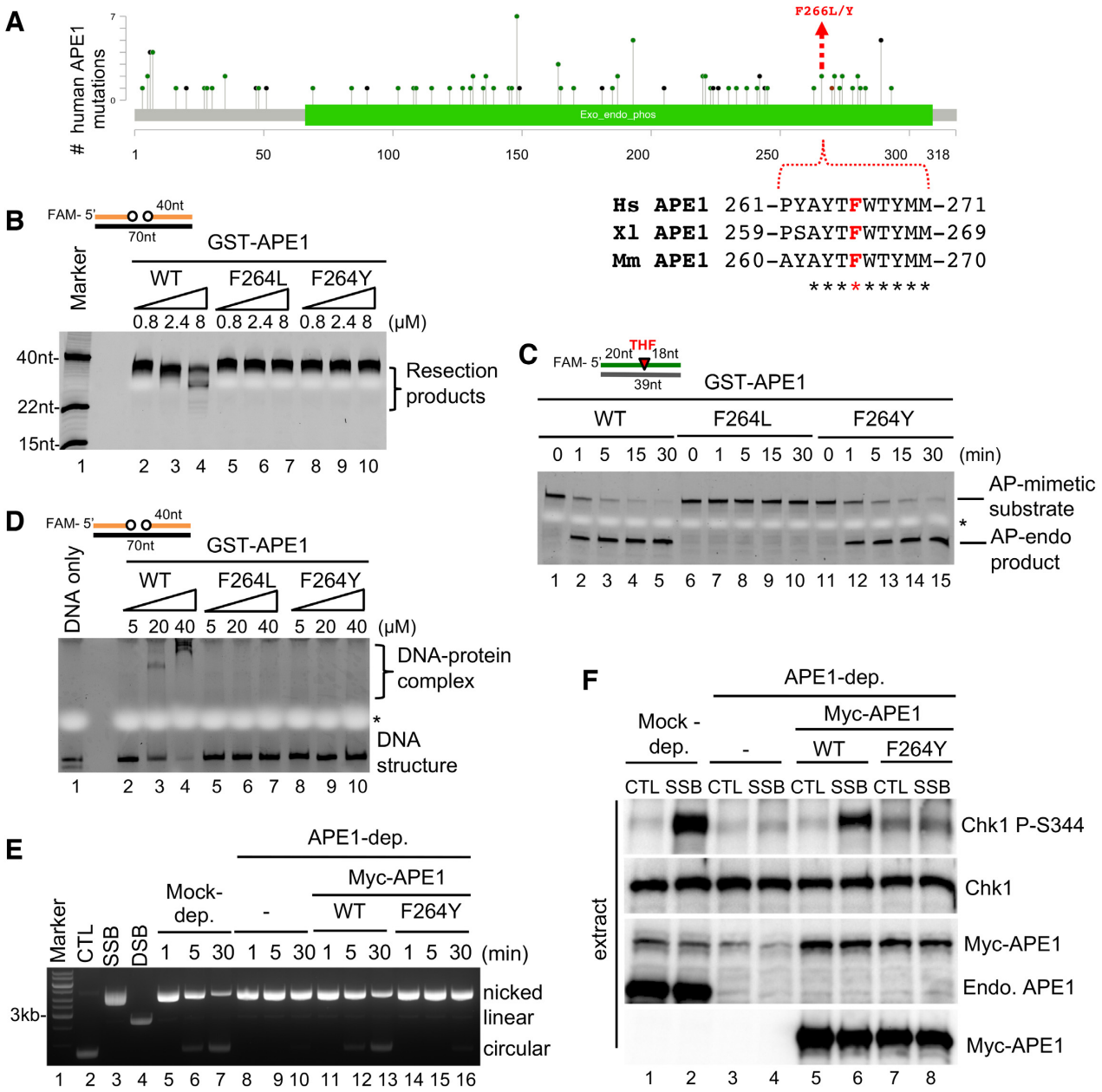

Figure 6. Characterization of patient-derived APE1 variants in SSB repair and signaling. (**A**) CBiolPortal analysis of human APE1 mutations from cancer patients. The F266L and F266Y mutations in human APE1 were identified in data from a cancer patient. A comparison of the sequences of the peptide surrounding the F266 residue in human (Hs), frog (Xl) and mouse (Mm) APE1 is shown under the schematic diagram. (**B**) The dsDNA–SSB structure was used to characterize the exonuclease activities of WT, F264L, and F264Y APE1 at different concentrations. (**C**) The endonuclease activities of WT, F264L and F264Y APE1 protein (0.08 μM) were examined *in vitro* using the dsDNA–AP as a substrate. (**D**) An EMSA shows the interaction between WT, F264L and F264Y APE1 and the dsDNA–AP–SSB structure *in vitro*. * nonspecific dye band from sample buffer in panels C and D. (**E**) The SSB plasmid was added to mock- or APE1-depleted HSS supplemented with WT or F264Y Myc-APE1. After different incubation times, the DNA repair products were isolated and analyzed on an agarose gel. (**F**) WT or F264Y Myc-APE1 was added back to APE1-depleted HSS supplemented with CTL or SSB plasmid. After incubation for 30 min, total egg extract were examined via immunoblotting analysis as indicated.

compared with that of WT APE1 (16,50). Human APE1 F266 corresponds to *Xenopus* APE1 F264 (Figure 6A). Intriguingly, we found that the 3′–5′ exonuclease activity of a *Xenopus* APE1 variant carrying a F264L or F264Y mutation was significantly compromised, although F264L and F264Y GST-APE1 proteins were purified similarly to the WT GST-APE1 (Figure 6B, Supplementary Figure S2A). On the other hand, the AP endonuclease activity of F264L APE1 (but not that of F264Y APE1) was lower than that of WT APE1 (Figure 6C). Thus, our observations revealed that a *Xenopus* APE1 variant carrying the F264Y mutation is deficient in exonuclease activity but proficient in AP endonuclease activity under the conditions we tested, highlighting the potential significance of APE1's exonucle-

ase activity in cancer etiology. EMSAs demonstrated that WT APE1 (but not F264L APE1 or F264Y APE1) interacts with the dsDNA–SSB structure *in vitro* (Figure 6D). We obtained similar results in EMSAs with the dsDNA–SSB–biotin and dsDNA–AP–SSB structures (Supplementary Figure S5D and E). These observations are consistent with the idea that SSB recognition by APE1 as well as its affinity for the SSB structure are important for its exonuclease activity.

What is the significance of the exo-deficient F264Y mutation in APE1 functions? Notably, WT Myc-APE1, but not F264Y Myc-APE1, rescued the repair of the SSB plasmid in APE1-depleted HSS (Figure 6E). Furthermore, WT Myc-APE1, but not F264Y Myc-APE1, rescued Chk1 phosphorylation induced by the defined SSB structure in APE1-depleted HSS (Figure 6F). These defects of the *Xenopus* APE1 F264Y variant in SSB repair and SSB signaling suggest that the human F266Y variant may be involved in cancer etiology via similar defects in SSB repair and signaling.

DISCUSSION

The results of this work provide evidence that APE1 senses and recognizes SSB sites to initiate SSB end resection. Thus, we propose a two-step model for SSB end resection in SSB repair and signaling (Figure 7): (**Step 1**) SSBs are first recognized by APE1 for the initiation of SSB end resection, and (**Step 2**) APE2 promotes the continuation of SSB end resection. APE1 senses SSBs and is recruited to SSB sites independently of APE2 (Figures 1–3). Next, APE1 initiates end resection in the 3′–5′ direction via its exonuclease activity to create a small ssDNA gap that may lead to APE1 dissociation and APE2 recruitment (Figures 3 and 4). A distinct Zf-GRF motif containing a CHCC Zn^{2+}-binding site and a conserved GRxF signature peptide in the C-terminus of APE2 interacts with ssDNA to promote its 3′–5′ exonucleas activty and SSB end resection (28–30). Thus, the ssDNA region at the gap structure induced by APE1-mediated initiation of SSB end resection may enhance APE2's exonuclease activity via a direct interaction with APE2's Zf-GRF motif, leading to the continuation of the 3′–5′ SSB end resection. Furthermore, APE1 interacts with APE2 and PCNA, which may also help the transition from APE1 to APE2 although the exact mechanism remains unclear (Figure 5).

We recently proposed the new concept of SSB end resection for genome integrity, which is composed of SSB end sensing as well as initiation, continuation, and termination of SSB end resection (34). It appears that APE2 contributes to the continuation but not the initiation of SSB end resection (30,34). We provide substantial evidence showing that APE1 senses SSBs to initiate SSB end resection via its distinct 3′–5′ exonuclease activity. Importantly, APE1 plays a previously uncharacterized but essential role in SSB end resection upstream of APE2. Similar to the significance of 5′–3′ DSB end resection for DSB repair and signaling (51,52), APE1-mediated 3′–5′ SSB end resection is also required for SSB repair and SSB signaling via distinct mechanisms though.

Our model suggests that APE2 may bind with a gap structure. To directly this directly, we prepared a 70-bp dsDNA with biotin on 5′-side of both strands (designated as biotin–dsDNA), a SSB structure in the defined location of the biotin–dsDNA (designated as biotin–dsDNA–SSB), and a gapped structure after biotin–dsDNA–SSB was resected *in vitro* (designated as biotin–dsDNA–gap). We then determined whether beads coupled with these biotin–labeled substrates can pulldown recombinant Myc-APE2 in a buffer *in vitro*. Interestingly, the recombinant Myc-APE2 was revealed on beads coupled with biotin–dsDNA–gap and biotin–dsDNA–SSB, but not just biotin–dsDNA nor no DNA, suggesting that APE2 can bind to a gap or SSB structure *in vitro* (Supplementary Figure S6C). This *in vitro* observation is reminiscent of a previous study characterizing *in vitro* exonuclease of recombinant human APE2 protein using both SSB and gap structures (48). Future studies may use more quantitative approach to compare association and dissociation of recombinant APE2 to different gap/SSB structures. Of note, APE2 cannot bind to the SSB plasmid in the APE1-depleted HSS (compare lanes 10–12 to lanes 4–6 in 'DNA-bound', Figure 1C), suggesting that APE2 binding to SSB site may be hampered by an unknown mechanism in the HSS system.

Why does APE1 couple SSB repair with SSB signaling? Prior studies have demonstrated that SSBs are detected and sensed by PARP1 (6,8) and that SSBs are repaired

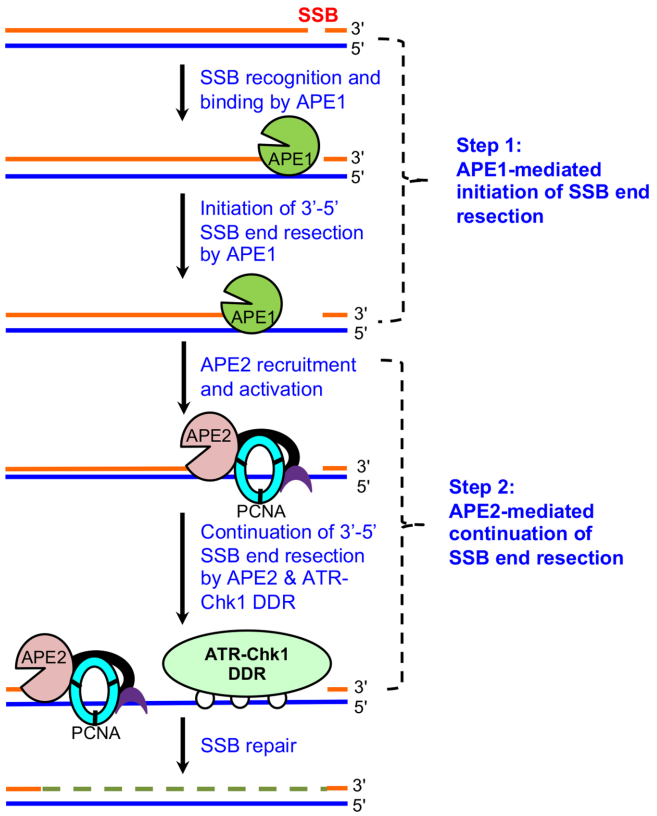

Figure 7. A two-step mechanism for SSB end resection in SSB repair and signaling. **Step 1:** An SSB is recognized by APE1, which then initiates SSB end resection in the 3′–5′ direction to generate a small gap (this work). **Step 2:** APE2 is recruited to the small gap likely via PCNA, and its exonuclease activity is activated and enhanced via several distinct regulatory mechanisms (28–30). After this two-step SSB end resection, the ATR–Chk1 DDR pathway is activated and the SSB is eventually repaired. See the text for more details.

by XRCC1-mediated repair pathway (1,7,9). However, neither PARP1 nor XRCC1 is required for activation of SSB-induced ATR–Chk1 DDR pathway (30). We provide evidence in this work that APE1 is required for both SSB repair and SSB signaling (Figures 1–6). It has been demonstrated that APE1 recognizes a 1-nt gap SSB structure to suppress PARP1 binding and activation in *in vitro* and mammalian cell-based *in vivo* experiments (53) and that APE1 facilitates the dissociation of PARP1 from AP site and AP-derived SSB structure (54). Furthermore, APE1 overexpression in XRCC1-deficient cells can complement the defective repair of oxidative stress-derived SSBs (55). These studies are consistent with the significant role of APE1 as an early sensor of SSB for repair. In addition, it has been shown in non-dividing cells that ATR DDR pathway is activated by SSBs derived from UV-induced photolesions via APE1's endonuclease activity (56). To the best of our knowledge, our study is the first to provide direct evidence that APE1's exonuclease activity is required for SSB repair and signaling.

It is noted in *Xenopus* system that both APE1 and APE2 are engaged by the distinct SSB repair system to chew back non-damaged correctly based paired DNA instead of having a canonical SSB repair with a DNA polymerase and a ligase. What would cells choose the canonical SSB repair or the 3′–5′ end resection-mediated SSB repair? We speculate that cells may choose canonical SSB repair when the level of SSBs is under sort of a threshold, and that cells may switch to the 3′–5 end resection to trigger DNA damage checkpoint for more time to repair SSBs when the level of SSBs is above such threshold. Alternatively, cells may make choice of different SSB repair pathways depending on the cell cycle phase or the availability of repair proteins. It is interesting to test these different scenarios using cultured cell systems in future studies.

APE1 plays essential roles in genome integrity via its AP endonuclease activity and redox regulation of transcription (14,57). In this work, we provide direct evidence showing the significance of APE1's exonuclease activity for SSB repair and signaling. APE1 senses and processes SSB to initiate SSB end resection via its exonuclease activity, suggesting an indispensable role of APE1 for genome stability. In particular, we have characterized the phenotype of two APE1 variants (carrying either DA mutant or F266Y mutant) with defective exonuclease activity but normal endonuclease activity under the conditions we tested. Furthermore, a recent study demonstrated that the increased exonuclease activity of the human F266A APE1 variant is due to a conformational change in its active site that occurs when it is complexed with its DNA substrate (50). Future structural studies are needed to reveal the molecular details of how the F264Y mutant impairs APE1's exonuclease activity. In addition, our EMSA results show APE1's preferential binding to two defined SSB structures *in vitro* (Figure 3A and B), which was compromised in DA or CA APE1 (Figure 3C and D). The deficiency of DA APE1 binding to SSB structure was confirmed with another more quantitative approach MST assay (Figure 3E). A prior study showed that human APE1 carrying D308A mutant bound to an incised AP site-containing substrate *in vitro* in a similar fashion to WT APE1 (58). The discrepancy of this study with our observation may be because of different substrates or experimental conditions. Consistent with our observations, another study using molecular modeling revealed that D308A APE1 can't make proper contact with DNA substrate (43).

Although both APE1 and APE2 display exonuclease activity, their regulation and activation are quite different from each other. APE2 interacts with PCNA via two distinct modes, which stimulates its exonuclease activity (30,47,59). PCNA interacts with APE1 directly; however, PCNA is dispensable for APE1's exonuclease activity (Supplementary Figure S7), suggesting that PCNA plays differential role for the activation of APE1 and APE2 exonuclease activity. Previous studies have shown that PCNA interacts with APE1 and that they co-localize in nuclei (60,61). Furthermore, APE1 also interacts with APE2 directly (Figure 5). Although the exact mechanism is unclear, we speculate that APE1 interacts with PCNA and APE2 to facilitate the transition from the initiation to the continuation of SSB end resection.

Because of its abnormal expression and subcellular localization in numerous cancers, APE1 has been implicated in the development of resistance to cancer chemo- and radiotherapy; thus, APE1 represents an emerging therapeutic target for the treatment of various cancers (57,62,63). The deficiency of the patient-derived APE1 mutant (F264Y) for SSB repair and signaling (Figure 6) highlights the potential role of APE1 exonuclease activity for cancer etiology. Future work is needed to test this possibility directly using mouse models.

Taken together, our findings in this study provide evidence for the significance of APE1, and its exonuclease activity in particular, in SSB repair and signaling. Therefore, our research has shed new light on the significance of APE1 in the maintenance of genome stability.

SUPPLEMENTARY DATA

Supplementary Data are available at NAR Online.

ACKNOWLEDGEMENTS

We thank Drs Matthew Michael, Karlene Cimprich, Howard Lindsay, Scott Williams, Zhongsheng You and Doug Golenbock for reagents. We are grateful for the assistance by Dr Irina Nesmelova for MST analysis. We also thank Drs Yvette Huet and Chandra Williams as well as Vivarium staff for maintaining the health of our frogs.
Author contributions: Y.L., J.R. and S.Y. designed experiments. Y.L., J.R., J.L., A.H., M.A.H. and S.Y. performed experiments. Y.L., J.R., C.R., P.M. and S.Y. analyzed the data. S.Y. wrote the manuscript with the input from the other authors.

FUNDING

National Institute of General Medical Sciences of the National Institutes of Health [R15GM101571 and R15GM114713 to S.Y.]; National Cancer Institute of the National Institutes of Health [R01CA225637 to S.Y.]; National Institutes of Health [S10OD026970 for S.Y. as major user]; National Science Foundation [REU grant no. 1359271 for J.R. and A.H.]; Graduate School Summer Fellowship (GSSF) program at UNC Charlotte [to M.A.H.].

Funding for open access charge: National Institutes of Health.
Conflict of interest statement. None declared.

REFERENCES

1. Caldecott,K.W. (2008) Single-strand break repair and genetic disease. *Nat. Rev. Genet.*, **9**, 619–631.
2. Friedberg,E.C. (2003) DNA damage and repair. *Nature*, **421**, 436–440.
3. Tubbs,A. and Nussenzweig,A. (2017) Endogenous DNA damage as a source of genomic instability in cancer. *Cell*, **168**, 644–656.
4. Ciccia,A. and Elledge,S.J. (2010) The DNA damage response: making it safe to play with knives. *Mol. Cell*, **40**, 179–204.
5. Davis,L. and Maizels,N. (2014) Homology-directed repair of DNA nicks via pathways distinct from canonical double-strand break repair. *Proc. Natl. Acad. Sci. U.S.A.*, **111**, E924–E932.
6. Tallis,M., Morra,R., Barkauskaite,E. and Ahel,I. (2014) Poly(ADP-ribosyl)ation in regulation of chromatin structure and the DNA damage response. *Chromosoma*, **123**, 79–90.
7. Hanssen-Bauer,A., Solvang-Garten,K., Akbari,M. and Otterlei,M. (2012) X-ray repair cross complementing protein 1 in base excision repair. *Int. J. Mol. Sci.*, **13**, 17210–17229.
8. Eustermann,S., Wu,W.F., Langelier,M.F., Yang,J.C., Easton,L.E., Riccio,A.A., Pascal,J.M. and Neuhaus,D. (2015) Structural basis of detection and signaling of DNA single-strand breaks by human PARP-1. *Mol. Cell*, **60**, 742–754.
9. Brem,R. and Hall,J. (2005) XRCC1 is required for DNA single-strand break repair in human cells. *Nucleic Acids Res.*, **33**, 2512–2520.
10. McKinnon,P.J. and Caldecott,K.W. (2007) DNA strand break repair and human genetic disease. *Annu. Rev. Genomics Hum. Genet.*, **8**, 37–55.
11. Yan,S., Sorrell,M. and Berman,Z. (2014) Functional interplay between ATM/ATR-mediated DNA damage response and DNA repair pathways in oxidative stress. *Cell Mol. Life Sci.*, **71**, 3951–3967.
12. Nassour,J., Martien,S., Martin,N., Deruy,E., Tomellini,E., Malaquin,N., Bouali,F., Sabatier,L., Wernert,N., Pinte,S. *et al.* (2016) Defective DNA single-strand break repair is responsible for senescence and neoplastic escape of epithelial cells. *Nat. Commun.*, **7**, 10399.
13. Boiteux,S. and Guillet,M. (2004) Abasic sites in DNA: repair and biological consequences in Saccharomyces cerevisiae. *DNA Repair (Amst.)*, **3**, 1–12.
14. Tell,G., Quadrifoglio,F., Tiribelli,C. and Kelley,M.R. (2009) The many functions of APE1/Ref-1: not only a DNA repair enzyme. *Antioxid Redox Signal*, **11**, 601–620.
15. Wilson,D.M. 3rd and Barsky,D. (2001) The major human abasic endonuclease: formation, consequences and repair of abasic lesions in DNA. *Mutat. Res.*, **485**, 283–307.
16. Hadi,M.Z., Ginalski,K., Nguyen,L.H. and Wilson,D.M. 3rd. (2002) Determinants in nuclease specificity of Ape1 and Ape2, human homologues of Escherichia coli exonuclease III. *J. Mol. Biol.*, **316**, 853–866.
17. Chohan,M., Mackedenski,S., Li,W.M. and Lee,C.H. (2015) Human apurinic/apyrimidinic endonuclease 1 (APE1) has 3′ RNA phosphatase and 3′ exoribonuclease activities. *J. Mol. Biol.*, **427**, 298–311.
18. Whitaker,A.M. and Freudenthal,B.D. (2018) APE1: a skilled nucleic acid surgeon. *DNA Repair (Amst.)*, **71**, 93–100.
19. Xanthoudakis,S., Smeyne,R.J., Wallace,J.D. and Curran,T. (1996) The redox/DNA repair protein, Ref-1, is essential for early embryonic development in mice. *Proc. Natl. Acad. Sci. U.S.A.*, **93**, 8919–8923.
20. Fung,H. and Demple,B. (2005) A vital role for Ape1/Ref1 protein in repairing spontaneous DNA damage in human cells. *Mol. Cell*, **17**, 463–470.
21. Li,M. and Wilson,D.M. 3rd. (2014) Human apurinic/apyrimidinic endonuclease 1. *Antioxid. Redox Signal.*, **20**, 678–707.
22. Wu,R.A., Semlow,D.R., Kamimae-Lanning,A.N., Kochenova,O.V., Chistol,G., Hodskinson,M.R., Amunugama,R., Sparks,J.L., Wang,M., Deng,L. *et al.* (2019) TRAIP is a master regulator of DNA interstrand crosslink repair. *Nature*, **567**, 267–272.
23. Kumagai,A., Lee,J., Yoo,H.Y. and Dunphy,W.G. (2006) TopBP1 activates the ATR-ATRIP complex. *Cell*, **124**, 943–955.
24. Lin,Y., Ha,A. and Yan,S. (2019) Methods for studying DNA single-strand break repair and signaling in Xenopus laevis egg extracts. *Methods Mol. Biol.*, **1999**, 161–172.
25. Lebofsky,R., Takahashi,T. and Walter,J.C. (2009) DNA replication in nucleus-free Xenopus egg extracts. *Methods Mol. Biol.*, **521**, 229–252.
26. Willis,J., DeStephanis,D., Patel,Y., Gowda,V. and Yan,S. (2012) Study of the DNA damage checkpoint using Xenopus egg extracts. *J. Vis. Exp.*, e4449.
27. Cupello,S., Richardson,C. and Yan,S. (2016) Cell-free Xenopus egg extracts for studying DNA damage response pathways. *Int. J. Dev. Biol.*, **60**, 229–236.
28. Willis,J., Patel,Y., Lentz,B.L. and Yan,S. (2013) APE2 is required for ATR-Chk1 checkpoint activation in response to oxidative stress. *Proc. Natl. Acad. Sci. U.S.A.*, **110**, 10592–10597.
29. Wallace,B.D., Berman,Z., Mueller,G.A., Lin,Y., Chang,T., Andres,S.N., Wojtaszek,J.L., DeRose,E.F., Appel,C.D., London,R.E. *et al.* (2017) APE2 Zf-GRF facilitates 3′-5′ resection of DNA damage following oxidative stress. *Proc. Natl. Acad. Sci. U.S.A.*, **114**, 304–309.
30. Lin,Y., Bai,L., Cupello,S., Hossain,M.A., Deem,B., McLeod,M., Raj,J. and Yan,S. (2018) APE2 promotes DNA damage response pathway from a single-strand break. *Nucleic Acids Res.*, **46**, 2479–2494.
31. Li,F., Wang,Q., Seol,J.H., Che,J., Lu,X., Shim,E.Y., Lee,S.E. and Niu,H. (2019) Apn2 resolves blocked 3′ ends and suppresses Top1-induced mutagenesis at genomic rNMP sites. *Nat. Struct. Mol. Biol.*, **26**, 155–163.
32. Yan,S. (2019) Resolution of a complex crisis at DNA 3′ termini. *Nat. Struct. Mol. Biol.*, **26**, 335–336.
33. Mengwasser,K.E., Adeyemi,R.O., Leng,Y., Choi,M.Y., Clairmont,C., D'Andrea,A.D. and Elledge,S.J. (2019) Genetic screens reveal FEN1 and APEX2 as BRCA2 synthetic lethal targets. *Mol. Cell*, **73**, 885–899.
34. Hossain,M.A., Lin,Y. and Yan,S. (2018) Single-strand break end resection in genome integrity: mechanism and regulation by APE2. *Int. J. Mol. Sci.*, **19**, 2389.
35. Yan,S. and Michael,W.M. (2009) TopBP1 and DNA polymerase-alpha directly recruit the 9-1-1 complex to stalled DNA replication forks. *J. Cell Biol.*, **184**, 793–804.
36. Wilson,D.M. 3rd. (2003) Properties of and substrate determinants for the exonuclease activity of human apurinic endonuclease Ape1. *J. Mol. Biol.*, **330**, 1027–1037.
37. Lupardus,P.J. and Cimprich,K.A. (2006) Phosphorylation of Xenopus Rad1 and Hus1 defines a readout for ATR activation that is independent of Claspin and the Rad9 carboxy terminus. *Mol. Biol. Cell*, **17**, 1559–1569.
38. Jones,R.E., Chapman,J.R., Puligilla,C., Murray,J.M., Car,A.M., Ford,C.C. and Lindsay,H.D. (2003) XRad17 is required for the activation of XChk1 but not XCds1 during checkpoint signaling in Xenopus. *Mol. Biol. Cell*, **14**, 3898–3910.
39. Rai,G., Vyjayanti,V.N., Dorjsuren,D., Simeonov,A., Jadhav,A., Wilson,D.M. 3rd and Maloney,D.J. (2012) Synthesis, biological evaluation, and structure-activity relationships of a novel class of apurinic/apyrimidinic endonuclease 1 inhibitors. *J. Med. Chem.*, **55**, 3101–3112.
40. Madhusudan,S., Smart,F., Shrimpton,P., Parsons,J.L., Gardiner,L., Houlbrook,S., Talbot,D.C., Hammonds,T., Freemont,P.A., Sternberg,M.J. *et al.* (2005) Isolation of a small molecule inhibitor of DNA base excision repair. *Nucleic Acids Res.*, **33**, 4711–4724.
41. Bapat,A., Glass,L.S., Luo,M., Fishel,M.L., Long,E.C., Georgiadis,M.M. and Kelley,M.R. (2010) Novel small-molecule inhibitor of apurinic/apyrimidinic endonuclease 1 blocks proliferation and reduces viability of glioblastoma cells. *J. Pharmacol. Exp. Ther.*, **334**, 988–998.
42. Kelley,M.R., Georgiadis,M.M. and Fishel,M.L. (2012) APE1/Ref-1 role in redox signaling: translational applications of targeting the redox function of the DNA repair/redox protein APE1/Ref-1. *Curr. Mol. Pharmacol.*, **5**, 36–53.
43. Wang,Z., Ayoub,E., Mazouzi,A., Grin,I., Ishchenko,A.A., Fan,J., Yang,X., Harihar,T., Saparbaev,M. and Ramotar,D. (2014) Functional variants of human APE1 rescue the DNA repair defects of the yeast AP endonuclease/3′-diesterase-deficient strain. *DNA Repair (Amst.)*, **22**, 53–66.
44. Gelin,A., Redrejo-Rodriguez,M., Laval,J., Fedorova,O.S., Saparbaev,M. and Ishchenko,A.A. (2010) Genetic and biochemical

characterization of human AP endonuclease 1 mutants deficient in nucleotide incision repair activity. *PLoS One*, **5**, e12241.
45. McNeill,D.R. and Wilson,D.M. 3rd. (2007) A dominant-negative form of the major human abasic endonuclease enhances cellular sensitivity to laboratory and clinical DNA-damaging agents. *Mol. Cancer Res.*, **5**, 61–70.
46. Freudenthal,B.D., Beard,W.A., Cuneo,M.J., Dyrkheeva,N.S. and Wilson,S.H. (2015) Capturing snapshots of APE1 processing DNA damage. *Nat. Struct. Mol. Biol.*, **22**, 924–931.
47. Burkovics,P., Hajdu,I., Szukacsov,V., Unk,I. and Haracska,L. (2009) Role of PCNA-dependent stimulation of 3′-phosphodiesterase and 3′-5′ exonuclease activities of human Ape2 in repair of oxidative DNA damage. *Nucleic Acids Res.*, **37**, 4247–4255.
48. Burkovics,P., Szukacsov,V., Unk,I. and Haracska,L. (2006) Human Ape2 protein has a 3′-5′ exonuclease activity that acts preferentially on mismatched base pairs. *Nucleic Acids Res.*, **34**, 2508–2515.
49. Unk,I., Haracska,L., Gomes,X.V., Burgers,P.M., Prakash,L. and Prakash,S. (2002) Stimulation of 3′→5′ exonuclease and 3′-phosphodiesterase activities of yeast apn2 by proliferating cell nuclear antigen. *Mol. Cell Biol.*, **22**, 6480–6486.
50. Whitaker,A.M., Flynn,T.S. and Freudenthal,B.D. (2018) Molecular snapshots of APE1 proofreading mismatches and removing DNA damage. *Nat. Commun.*, **9**, 399.
51. Daley,J.M., Niu,H., Miller,A.S. and Sung,P. (2015) Biochemical mechanism of DSB end resection and its regulation. *DNA Repair (Amst.)*, **32**, 66–74.
52. Symington,L.S. (2014) End resection at double-strand breaks: mechanism and regulation. *Cold Spring Harbor Perspect. Biol.*, **6**, a016436.
53. Peddi,S.R., Chattopadhyay,R., Naidu,C.V. and Izumi,T. (2006) The human apurinic/apyrimidinic endonuclease-1 suppresses activation of poly(adp-ribose) polymerase-1 induced by DNA single strand breaks. *Toxicology*, **224**, 44–55.
54. Liu,L., Kong,M., Gassman,N.R., Freudenthal,B.D., Prasad,R., Zhen,S., Watkins,S.C., Wilson,S.H. and Van Houten,B. (2017) PARP1 changes from three-dimensional DNA damage searching to one-dimensional diffusion after auto-PARylation or in the presence of APE1. *Nucleic Acids Res.*, **45**, 12834–12847.
55. Sossou,M., Flohr-Beckhaus,C., Schulz,I., Daboussi,F., Epe,B. and Radicella,J.P. (2005) APE1 overexpression in XRCC1-deficient cells complements the defective repair of oxidative single strand breaks but increases genomic instability. *Nucleic Acids Res.*, **33**, 298–306.
56. Vrouwe,M.G., Pines,A., Overmeer,R.M., Hanada,K. and Mullenders,L.H. (2011) UV-induced photolesions elicit ATR-kinase-dependent signaling in non-cycling cells through nucleotide excision repair-dependent and -independent pathways. *J. Cell Sci.*, **124**, 435–446.
57. Fishel,M.L. and Kelley,M.R. (2007) The DNA base excision repair protein Ape1/Ref-1 as a therapeutic and chemopreventive target. *Mol. Aspects Med.*, **28**, 375–395.
58. Masuda,Y., Bennett,R.A. and Demple,B. (1998) Dynamics of the interaction of human apurinic endonuclease (Ape1) with its substrate and product. *J. Biol. Chem.*, **273**, 30352–30359.
59. Tsuchimoto,D., Sakai,Y., Sakumi,K., Nishioka,K., Sasaki,M., Fujiwara,T. and Nakabeppu,Y. (2001) Human APE2 protein is mostly localized in the nuclei and to some extent in the mitochondria, while nuclear APE2 is partly associated with proliferating cell nuclear antigen. *Nucleic Acids Res.*, **29**, 2349–2360.
60. Jung,H.J., Kim,E.H., Mun,J.Y., Park,S., Smith,M.L., Han,S.S. and Seo,Y.R. (2007) Base excision DNA repair defect in Gadd45a-deficient cells. *Oncogene*, **26**, 7517–7525.
61. Dianova,II, Bohr,V.A. and Dianov,G.L. (2001) Interaction of human AP endonuclease 1 with flap endonuclease 1 and proliferating cell nuclear antigen involved in long-patch base excision repair. *Biochemistry*, **40**, 12639–12644.
62. Abbotts,R. and Madhusudan,S. (2010) Human AP endonuclease 1 (APE1): from mechanistic insights to druggable target in cancer. *Cancer Treat. Rev.*, **36**, 425–435.
63. Thakur,S., Sarkar,B., Cholia,R.P., Gautam,N., Dhiman,M. and Mantha,A.K. (2014) APE1/Ref-1 as an emerging therapeutic target for various human diseases: phytochemical modulation of its functions. *Exp. Mol. Med.*, **46**, e106.